Assessment of turbulence-chemistry interaction models in the computation of turbulent non-premixed flames

M T Lewandowski[1,2] **and J Pozorski**[1]

[1] Institute of Fluid-Flow Machinery, Polish Academy of Sciences, Gdańsk, Poland
[2] Conjoint Doctoral School of Gdańsk University of Technology and IFFM, Gdańsk, Poland

E-mail: michal.lewandowski@imp.gda.pl, jp@imp.gda.pl

Abstract. The present work reports on the assessment of different turbulence-chemistry interaction closures for the modelling of turbulent non-premixed combustion. Two-dimensional axisymmetric simulations have been carried out based on three different laboratory flames. The methane fueled, piloted jet flame Sandia D, the simple jet syngas flame and the so-called Delft Jet-in-Hot Coflow flame are studied. All the flames can be characterised as non-premixed but differ by some features which are taken into account through appropriate modelling approach.

1. Introduction

Turbulent combustion is an interdisciplinary and broad topic. It combines turbulent flow, described by the fluid dynamics equations, and complex chemical kinetics. Turbulence enhances mixing of the reactants; on the other hand, the chemical reactions, involving the temperature rise, change density and affect the flow itself. Therefore, aside of mass and heat transfer (including radiation), the coupling between turbulence and chemistry plays a crucial role in turbulent reactive flows. Due to the multi-scale character of the phenomena in space and time [1], combustion appears as a challenging task for numerical predictions. Nowadays, computational tools are of great importance for the design of fluid-flow machinery [2]. The accurate control of turbulent flames is required, e.g., to meet the environmental restrictions on the air pollution emissions, for optimal combustion chamber design, and for the safety issues. Development of various alternative technologies can be observed in the fields of combustion systems in the energy industry. Examples are fluidized bed combustors, oxy-fuel combustion, Moderate and Intense Low Oxygen Dilution (MILD) combustion or technologies based on production and utilization of low calorific gas from biomass or different kind of waste.

The Reynolds-Averaged (RANS) methods have been widely used in industrial applications for more than 20 years. Now, due to the increase in computational capabilities, the Large Eddy Simulations (LES) are getting more popular as well. The unsteady effects are meaningful in the reactive flows, especially in complex geometries of engines or turbine combustion chambers. Therefore, the LES method seems to be much more suitable than the RANS. Although the turbulent combustion including complex chemical mechanisms is still computationally very expensive, the LES method is being applied and developed in real life applications by world leading research institutions supported by the top automotive and aerospace industries.


Content from this work may be used under the terms of the Creative Commons Attribution 3.0 licence. Any further distribution of this work must maintain attribution to the author(s) and the title of the work, journal citation and DOI.
Published under licence by IOP Publishing Ltd

However, in many technical applications of local industry the cost of LES approach for combustion is prohibitive, therefore we still see the need of development for RANS methods, especially in case of specific conditions resulting from the use of new low calorific fuels or technologies such as MILD combustion. The need for comprehensive understanding of combustion leads to the study of chemical reactions in flames using experimental and numerical tools. Experimental investigations that aim for numerical model validation are often conducted on the flames issuing from the laboratory burners with the use of laser diagnostic techniques. In this work we present a numerical study of three non-premixed flames and an assessment of four turbulence-chemistry interaction (TCI) models with the use of AnsysFluent (AF) and OpenFOAM (OF) CFD codes.

2. Theory and modelling

2.1. Turbulent flow and turbulence-chemistry interaction

In order to deal with the problem of turbulent reactive flow, one has to solve the system of closed equations of motion, species transport and energy conservation [3]. In the present work the Navier-Stokes equations are subject to decomposition and Favre averaging. The closure for the turbulent fluxes can be obtained by statistical modelling based on turbulent viscosity which can be calculated as $\mu_t = \bar{\rho}\nu_t = C_\mu \bar{\rho} k^2/\epsilon$. The turbulent scalar fluxes are modelled with a gradient closure. The turbulence kinetic energy k and its dissipation rate ϵ are obtained with a two equation $k-\epsilon$ turbulence model [4]. The key difficulty in mathematical modelling of turbulent combustion is the source therm in the species transport equation. The reaction rate is based on the Arrhenius law which is highly non-linear, and it is not easy to express it as a function of mean values. Expanding the mean reaction rate as a Taylor series of the temperature fluctuation leads to various difficulties and is not commonly used [3]. Therefore existing models are based on physical analysis, comparing chemical and turbulent time scales, and most of them can be classified as one-point statistics, geometrical analysis or turbulent mixing approach [2].

2.1.1. Assumed Probability Density Function. It is one of the simplest approaches for TCI. The idea lies behind defining a mixture fraction ξ in the way that it is linked with instantaneous mass fractions Y_k in the relation $Y_k(\xi)$ and takes values 0 in the oxidizer stream inlet and 1 at the fuel inlet. This approach is valid for infinitely fast, irreversible chemistry and the Lewis number equal to one. Then, the mean species mass fractions $k = 1, ..., N$ are obtained from [3]:

$$\bar{\rho}\tilde{Y}_k = \int_0^1 Y_k(\xi)\rho(\xi)p(\xi)d\xi, \tag{1}$$

where $p(\xi)$ is the probability density function which is often assumed to be parameterised by the mean mixture fraction and its second moment (the mixture fraction variance). Then instead of N species mass fraction transport equations only those for $\widetilde{\xi}$ and $\widetilde{\xi''^2}$ are solved.

2.1.2. Steady Laminar Flamelet. This model assumes that the structure of turbulent flame can be reconstructed by one-dimensional laminar flames embedded in a turbulent flow [5]. In order to do that, a so-called flamelet equation needs to be solved for a laminar flame:

$$\rho\frac{\partial Y_k}{\partial t} = \frac{1}{2}\rho\chi\frac{\partial^2 Y_k}{\partial \xi^2} + R_k \tag{2}$$

where $\chi = 2D(\nabla\xi)^2$ is the scalar dissipation rate, and its stoichiometric value may be used as a parameter for correct representation of the turbulent flow. The local derivative is neglected in a steady state approach. Then, functions $Y_k(\xi, \chi_{st})$ are stored in the flamelet libraries [3] and used to evaluate mean values of mass fractions similarly to equation (1).

2.1.3. Eddy Dissipation Concept. The EDC is based on turbulent mixing approach. The idea is that the reactions take place there where the reactants are mixed at the molecular level and the turbulence energy dissipation takes place in so-called fine structures whose size is of the order of the Kolmogorov scale [6, 7]. Fine scales are determined through the cascade model of energy dissipation [8] from larger to smaller scales with the use of turbulence model quantities, e.g. k and ϵ. Then the relations for the mass transfer rate $\dot{m}^*$ between fine structures and their surroundings (divided by the fine-structure mass) and the ratio of the fine structure mass to the total mass γ^* are known. The final expression for the mean reaction rate is given as [7]:

$$\bar{R}_k = \frac{\bar{\rho}\gamma^*\dot{m}^*}{1-\gamma^*}({Y_k}^* - \widetilde{Y}_k), \tag{3}$$

where Y_k^* is a mass fraction of a specie k in the fine structure which should be obtained from the solution of ordinary differential equation describing the perfectly stirred reactor (PSR).

2.1.4. Partially Stirred Reactor Model. The PaSR model recalls a detailed chemistry approach of EDC [9]. Here each computational cell is also split into two zones: reacting and non-reacting. A reacting zone has a homogeneous composition which can be treated as PSR. The mean reaction rate for the species k is given by the following expression:

$$\bar{R}_k = \kappa_k R_k \tag{4}$$

where R_k is the reaction rate of the species according to the used kinetic mechanism. The reactive fractions κ_k depend on the chemical time scale τ_{ch} and the micro-mixing time scale τ_m.

3. Experimental flames

In the current study we have simulated three flames. A commonly studied piloted flame Sandia D and a simple jet syngas flame CHN case B are from the TNF Workshop data archive [10]. The third experiment has been conducted at the Delft University of Technology by Oldenhof et al. [11]. The scalar data of Sandia D are from the work of Barlow and Frank [12] at Sandia National Laboratories, whereas velocity measurements were done by Schneider et al. [13] at Darmstadt University of Technology. Corresponding measurements for the flame CHN were conducted by Barlow et al. [14] and Flury [15] at ETH Zurich, respectively. The characteristic features of the three flames are presented in table 1. For the flame Sandia D there are available axial and six radial measurements, for CHN B axial and five radial and for DJHC there are axial and six radial. Additionally in the case of CHN and DJHC velocity measurements were done at the jet exit and 3 mm above it, respectively. For the DJHC burner also the radial temperature profile was available. These data were used for inlet boundary conditions in the simulations. For the flame Sandia D the uniform values of velocity and temperature were set as a boundary condition on the pre-inlet pipe in order to achieve a proper profile. Grid size independence studies were performed in the all three cases. We have used RMS values to plot the error bars of the experimental data presented in the next sections.

Table 1. The characteristic parameters of the flames [12, 14, 11]: fuel composition, burner type, jet Reynolds number and diameter of the fuel nozzle.

	Sandia D	CHN B	DJHC
Fuel	25% CH_4, 75% air	40% CO, 30% H_2, 30% N_2	81% CH_4, 4% C_2H_6, 15% N_2
Type	Piloted jet flame	Simple jet flame	Jet-in-Hot-Coflow
Jet *Re*	22400	16700	4100
Nozzle d	7.2 mm	7.72 mm	4.5 mm

4. Results

We have run a large number of simulations for the three non-premixed flames from which we present only the chosen ones. We have focused on the axial and radial distributions of scalar values as well as on locating the position of the highest deterioration of the temperature value, which may be an important information of practical meaning in the real life applications. In table 2, simulation series are summarized together with the maximum error in temperature prediction with its relative error and position. In the following sections, quantitative results are shown for the axial and radial distributions of temperature, velocity and OH radical mass fraction.

Table 2. The locations of the highest deviations of numerical results of temperature from the experimental values together with the relative error obtained with different approaches on the three flames. AF and OF denote AnsysFluent and OpenFOAM simulation, respectively.

Flame	Solver	Turbulence model	TCI model	$[z/d; r/d]$	ΔT [K]	rel. err. [%]
SandiaD	AF	standard k-ϵ	β PDF	[15; 1.9]	818	122
	AF	standard k-ϵ	SL Flamelet	[15; 1.9]	835	125
	AF	realizable k-ϵ	EDC	[15; 1.9]	872	130
	AF	s. k-ϵ, $C_{\epsilon 1} = 1.6$	β PDF	[15; 1.7]	589	62
CHN B	AF	s. k-ϵ, $C_{\epsilon 1} = 1.587$	β PDF	[20; 2.3]	523	60
	AF	s. k-ϵ, $C_{\epsilon 1} = 1.587$	SL Flamelet	[20; 2.5]	499	66
	OF	standard k-ϵ	EDC	[20; 2.3]	715	83
	OF	standard k-ϵ	PaSR	[20; 2.3]	855	100
	AF	standard k-ϵ	β PDF	[20; 2.7]	771	124
DJHC	AF	realizable k-ϵ	EDC	[20; 2.9]	385	27
	AF	realizable k-ϵ	EDC modified	[20; 7.6]	147	21
	OF	standard k-ϵ	EDC	[13.3; 2.2]	329	25
	OF	standard k-ϵ	EDC modified	[13.3; 8.7]	173	34

4.1. Sandia D flame

Three different TCI models were used in the simulation of Sandia D, namely β pdf, steady laminar flamelet and the EDC. All were used within AF code on a 2352-cell 2-dimensional anxisymmetric grid with a steady state simulation [17]. SIMPLE algorithm was used for pressure-velocity coupling and a second order discretisation method were applied. In the case of β PDF a 17 species PDF table was created, the flamelet library was obtained with GRI 3.0 detailed chemical mechanism and skeletal mechanism for CH_4 with 41 reactions and 16 species was applied in case of EDC. For turbulence closure the two equation $k - \epsilon$ model was used for β PDF and flamelet and realizable $k - \epsilon$ in case of EDC. Additionally we have performed a simulation for β PDF with standard $k - \epsilon$ model with $C_{\epsilon 1}$ constant changed from 1.44 to 1.6

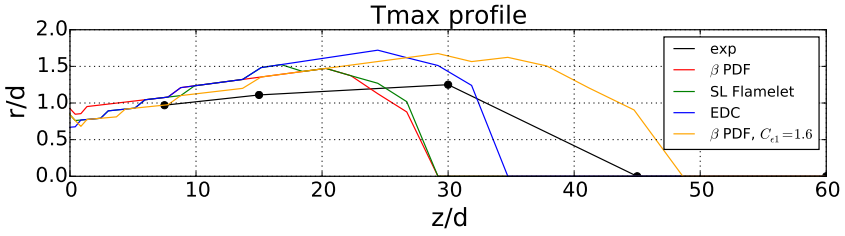

Figure 1. Positions of the peak temperature in the radial distributions presented in the non-dimensional axial and radial coordinates for the four simulations of the flame SandiaD.

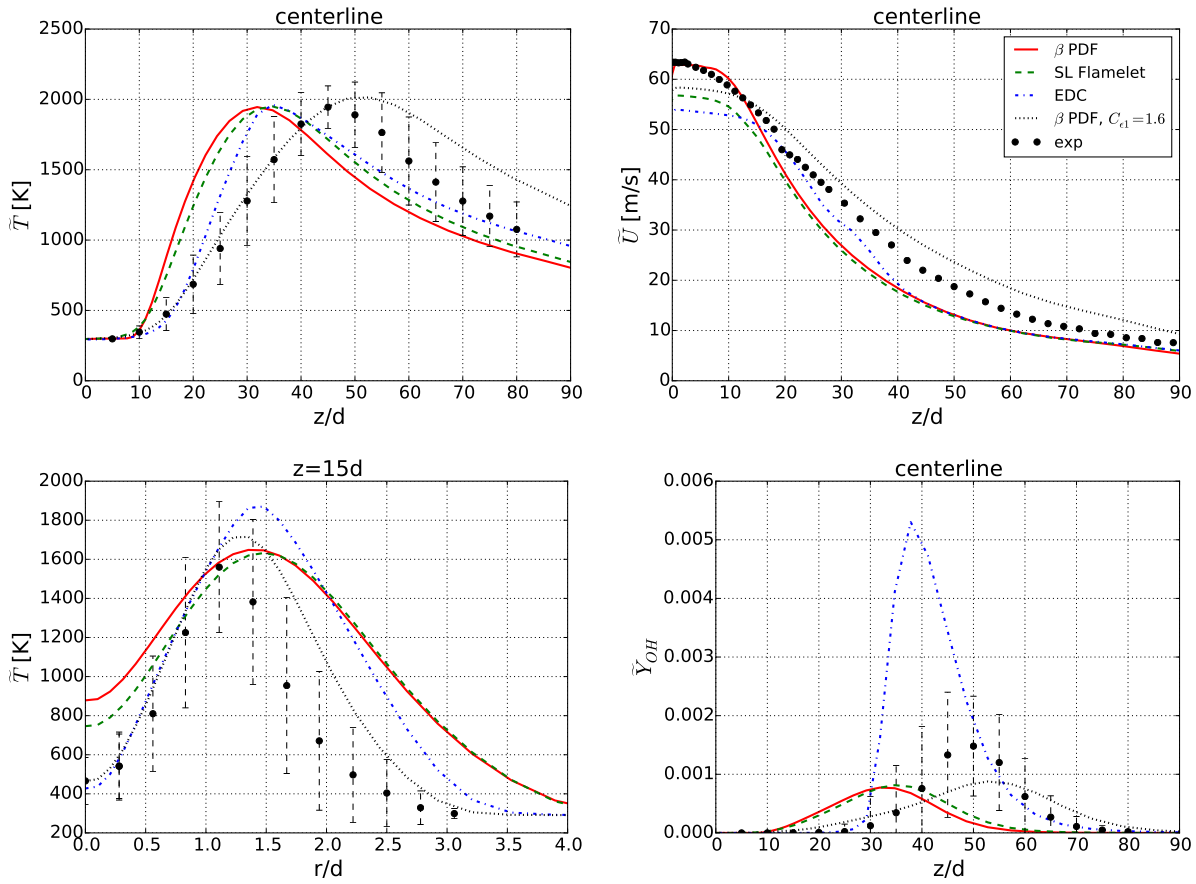

Figure 2. The results of simulations with AF for the flame Sandia D with three different turbulence-chemistry interaction models. The temperature distribution along the axis (top left) and the radial profile at the position $z = 15d$ (bottom left), the axial velocity values along the centerline (top right) and the mean mass fraction of OH radical (bottom right).

as it is common practice in the case of round jets [6, 16]. The effect of this correction is visible by a prediction of higher velocity values along the centerline in comparison to the standard model, what in fact shows better agreement with the experiment. On the other hand, it has a very strong impact on the axial temperature distribution by shifting the maximum value more downstream the flame. The upstream part predictions are very good but the downstream part temperature is slightly overestimated. Besides, predictions of the temperature distribution with the β PDF and flamelet models are quite similar whereas the EDC model shows a narrower profile of axial temperature what better corresponds to the experiment. The position of the maximum temperature might be adjusted with the use of $C_{\epsilon 1}$ constant as long as the flow results are in agreement with the experimental data. Results in fig. 1 show positions of the maximum temperature value in the radial distribution in the function of axial distance from the nozzle, what roughly indicates the flame zone and near stoichiometric region. It can be seen that the numerically predicted flame is always slightly wider and shorter without correction to $k - \epsilon$ model for the round jet. The mass fractions of OH radical distributions are predicted poorly with all the three models what is visible in fig. 2. For the β PDF and flamelet the maximum value in the axial distribution is underestimated whereas for the EDC it is highly overestimated. In the case of the latter model this might be improved by the use of a more detailed chemical mechanism.

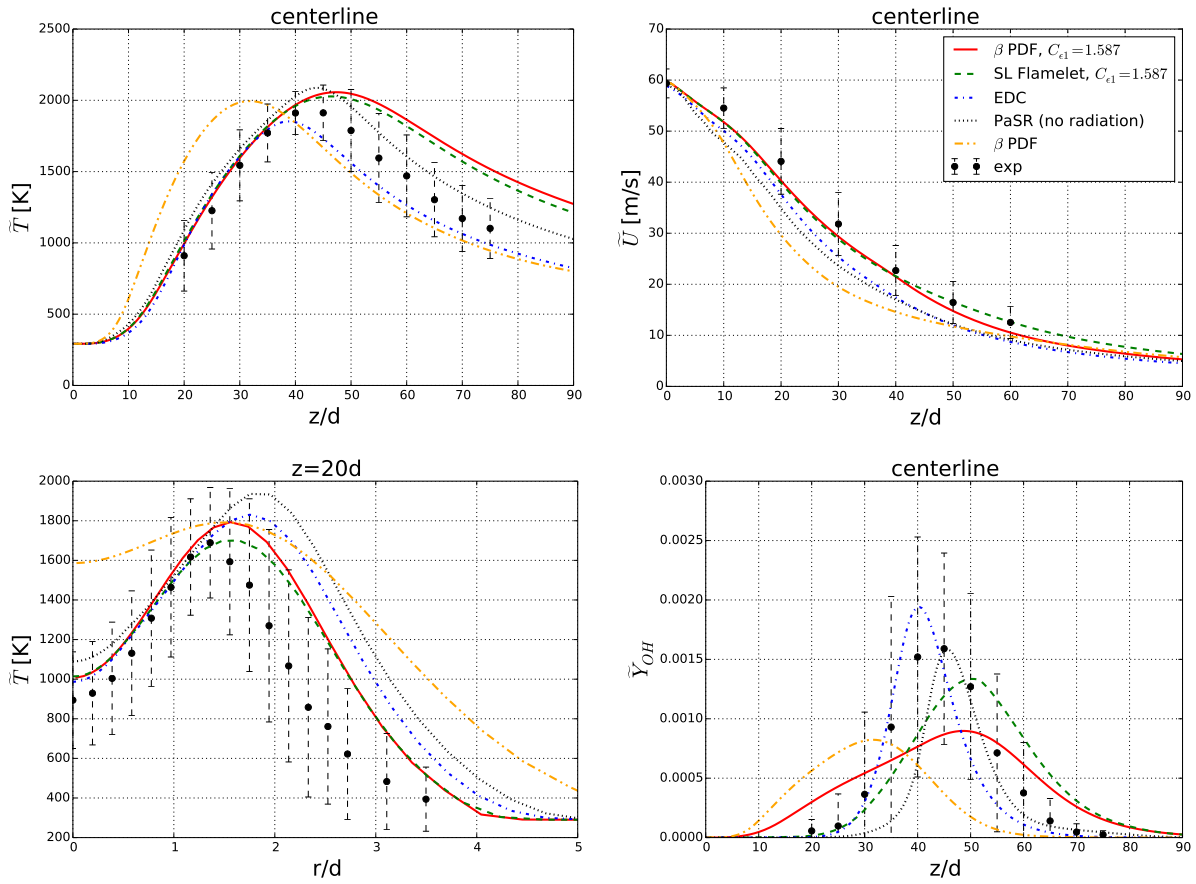

Figure 3. The results of AF and OF simulations for the syngas flame CHN B with four turbulence-chemistry interaction models. The temperature distribution along the axis (top left) and the radial profile at the position $z = 20d$ (bottom left), the axial velocity values along the centerline (top right) and the mean mass fraction of OH radical (bottom right).

4.2. Syngas CHN B flame

This flame was modelled with four TCI models: β pdf and steady laminar flamelet used within AF code and EDC and PaSR model used within OF code (edcPisoFoam [6] and reactingFoam solver, respectively). Simulations were carried out on axisymmetric 9949-cell grid as a steady state in AF and transient in OF [18]. Therefore the pressure-velocity coupling in the first case was done with the SIMPLE algorithm and with PISO in OF. In OF simulations a first-order implicit Euler method for the time integration was used and in all the simulations second order methods were used for space discretisation. The PDF table was constructed with 17 species and flamelet library was obtained with GRI 3.0 detailed chemical mechanism.

For the two mixing models, EDC and PaSR, several reduced chemical mechanisms were tested from which the optimal choice appeared to be the one proposed in [19] which consists of 13 species and 34 reactions. We have set the value of $C_{\epsilon 1}$ constant to 1.587 according to the formula given in [20]. This modification was applied to the AF simulations but not in case of OF where the corrected value of $C_{\epsilon 1}$ led to overestimation of the velocity centerline profile and drastically shifted the axial temperature distribution more downstream the jet leading to serious discrepancies from the experiment. The results are shown in fig. 3, where again the axial temperature distributions from β PDF method and SL flamelet are comparable. Similar situation was observed in the case of EDC and PaSR when no radiation model was applied.

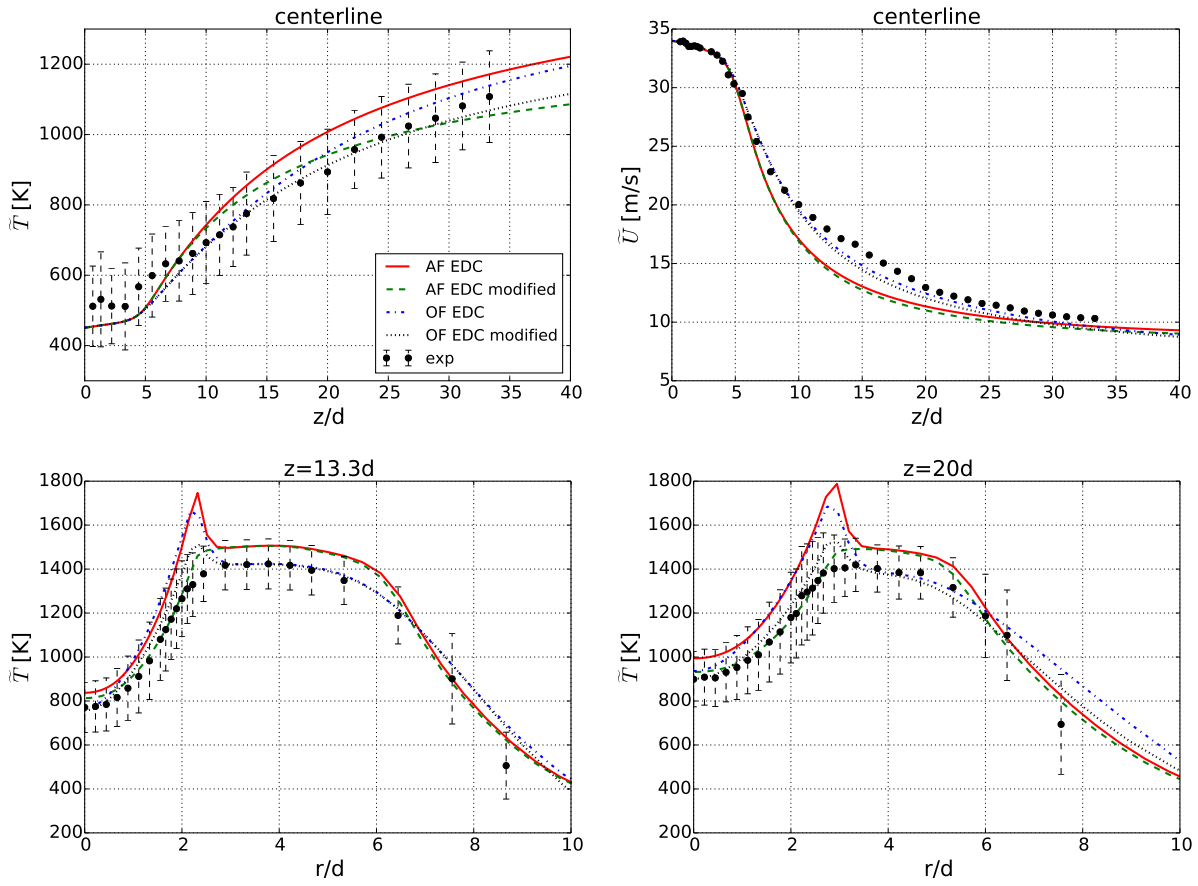

Figure 4. The EDC simulations results with AF nad OF for the flame DJHC-I $Re = 4100$ with and without modifications. The temperature distribution along the axis (top left) and two radial profiles at the position $z = 13.3d$ (bottom left) and $z = 20d$ (bottom right). Top right plot presents the axial velocity values along the centerline.

4.3. Delft-Jet-in-Hot-Coflow flame

Similar analysis as in the previous cases cannot be easily performed for the DJHC-I flame. Three different stream inlets are present here what would require the two mixture fraction approach. In MILD combustion regime the reaction rates are slower and the Damköhler number approaches unity. This requires including the finite rate chemistry. Besides, the reaction zone resembles well stirred reactor rather than laminar flamelets embedded in a turbulent flow. Therefore we have decided to use the EDC model with DRM19 chemical mechanism which consists of 19 species and 84 reactions as it proved to perform relatively well in MILD conditions in other investigations [16]. As it can be seen in fig. 4, the standard formulation of the EDC leads to a high overestimation of the peak temperature in the radial distributions. The specific features of MILD combustion are claimed [16] to be responsible for this effect. In order to overcome this problem, several modifications were proposed [16, 21, 22, 23] and most of them concern the change in the EDC model constants. We present the results of four simulations obtained with the two codes, AF and OF, with and without modifications. In the case of AF the modification concerns the change in EDC constants. Both values of C_γ and C_τ were changed to 1 and 3, respectively, as proposed by De et al. [16] and Evans et al. [21]. This approach, however, rises concerns about its generality and consistency with the turbulence models. Therefore in case of OF simulation we have applied clipping of γ^* greater than 0.5, what reduces the reaction rate for

low Reynolds numbers ($Re_\tau < 84$) but does not impact the model at fully turbulent conditions. It must be noted that due to the implementation differences this approach is not equivalent to the default clipping mentioned by De et al. [16] and discussed by Shiehnejadhesar et al. [24]. The adequacy of the proposed approaches is the subject of our other ongoing investigations. It should be also noted that the effect of radiation model in the case of OF simulation is stronger than in AF as evidenced by a lower temperature in the coflow region in radial distributions presented in fig 4. It is also found that both modifications reduce the peak value of the temperature so that the highest error is shifted off the jet to the outer edge of the coflow.

5. Conclusions

In general, the predictions of temperature for the Sandia D and CHN flames are in relatively good agreement with the experimental data for used TCI models. The highest deviations from the experiment occurred downstream the flame. Though, the largest temperature error was observed at the axial location 15-20 diameters downstream of the nozzle and 2.5-3 diameters off the jet axis for all the models. This is due to the shift of reaction zone more outside the axis upstream the jet and the predicted flames were wider. This discrepancy concerns the location of the flame zone and not the temperature value itself. In the case of DJHC burner this kind of deviation was not observed due to the presence of hot coflow. Yet, the maximum temperature was highly overestimated, what on the other hand was not the problem in the two previous flames. Two different modifications were applied to solve this problem: change in the EDC constants (as in the literature) and newly proposed clipping of γ^*. Additionally, we have observed some differences between the AF and OF results of velocity distributions that might be caused by the round jet configuration. As presented, the chosen TCI models are able to properly simulate different non-premixed flames that differ in fuel composition and specific features. The future work will focus on the modelling of combustion of low calorific fuels in MILD regime.

Acknowledgment

We are indebted to Prof. Dariusz Kardaś for his courtesy to access PC21 cluster for AnsysFluent runs. Calculations with OpenFOAM were carried out at the Academic Computer Centre in Gdańsk.

References

[1] Peters N 2009, *P. Combust. Inst.* **32** 1-25
[2] Veynante D and Vervisch L 2002 *Prog. Energ. Combust.* **28** 193-266
[3] Poinsot T and Veynante D 2012 *Theoretical and Numerical Combustion*, Third Edition, Bordeaux
[4] Launder B E and Spalding D B 1974 *Comput. Method. Appl. M.* **3** 269-289
[5] Peters N 2000 *Turbulent Combustion*, Cambridge University Press
[6] Lysenko D A, Ertesvåg I S and Rian K 2014 *Flow Turbul. Combust.* **93** 577-605
[7] Magnussen B 2005 *ECCOMAS Thematic Conference on Computational Combustion*, Lisbon
[8] Ertesvåg I S and Magnussen B F 2000 *Combust. Sci. Technol.* **159** 213-235
[9] Golovitchec V I and Chomiak J 2001 *The 4th International Symposium on HiTAC and Gasification*, Rome
[10] http://www.sandia.gov/TNF/abstract.html (10.06.2016)
[11] Oldenhof E, Tummers M J, van Veen E H and Roekaerts D J E M 2011 *Combust. Flame* **158** 1553-1563
[12] Barlow R S and Frank J H 1998 *P. Combust. Inst.* **27** 1087-1095
[13] Schneider Ch, Dreizler A, Janicka J and Hassel E P 2003 *Combust. Flame* **135** 185-190
[14] Barlow R S, Fiechtner G J, Cartner C D and Chen J Y 2000 *Combust. Flame* **120** 549-569
[15] Flury M 1998 *Exp. Analyse der Mischungstruktur in turbulent nicht vorgemischten Flammen* ETH Zurich
[16] De A, Oldenhof E, Sathiah P and Roekaerts D 2011 *Flow Turbul. Combust.* **87** 537-567
[17] Lewandowski M T and Pozorski J 2014 in Szewczyk M (Eds), *Applications of Thermodynamic Analysis in Description of Physical Phenomena In Energy Devices* (in Polish), OWPRz, Rzeszów
[18] Lewandowski M T and Pozorski J 2015 *P. Eur. Combust. Meet.* art. **P4-58**, Budapest
[19] Frassoldati A, Faravelli T and Ranzi E 2007 *Int. J. Hydrogen Energ.* **32**:3471-3485
[20] McGuirk J J and Rodi W 1979 *1st Symp. on Turbulent Shear Flows* 71-83, Pennsylvania State University
[21] Evans M J, Medwell P R and Tian Z F 2015 *Combust. Sci. Technol.* **187** 1093-1109
[22] Parente A, Malik M R, Cantino F, Cuoci A and Dally B B 2016 *Fuel* **163** 98-111
[23] Aminian J, Galletti C and Tognotti L 2016 *Fuel* **165** 123-133
[24] Shiehnejadhesar A, Scharler R, Goldin G M and Obernberger I 2014 *Fuel* **126** 177-187